TNP-8N_3-ADP Photoaffinity Labeling of Two Na,K-ATPase Sequences under Separate Na^+ plus K^+ Control†

Douglas G. Ward,‡,§ Mark Taylor,‡,∥ Kathryn S. Lilley,⊥,# and José D. Cavieres*,‡

Transport ATPase Laboratory, Department of Cell Physiology and Pharmacology, Faculty of Medicine and Biological Sciences, and Protein and Nucleic Acid Laboratory, University of Leicester, Leicester LE1 9HN, United Kingdom

Received September 22, 2005; Revised Manuscript Received December 7, 2005

ABSTRACT: ATP has high- and low-affinity effects on the sodium pump and other P-type ATPases. We have approached this question by using 2′,3′-*O*-(trinitrophenyl)-8-azidoadenosine 5′-diphosphate (TNP-8N_3-ADP) to photoinactivate and label Na,K-ATPase, both in its native state and after covalent FITC block of its high-affinity ATP site. With the native enzyme, the photoinactivation rate constant increases hyperbolically with a $K_{D(TNP-8N_3-ADP)}$ of 0.11 μM; TNP-ATP and ATP protect the site with high affinities. The inactivation does not require Na^+, but K^+ inhibits with a K_K' of 12 μM; Na^+ reverses this effect, with a K_{Na} of 0.17 mM. This pattern suggests that Na^+ and K^+ are binding at sites in their "intracellular" conformation. It was known that FITC did not abolish the reverse phosphorylation by P_i, or the K^+-phosphatase activity, and that TNP-8N_3-ADP could subsequently photoinactivate the latter with >100-fold lower affinity; in that case, the cation sites acted as if facing outward [Ward, D. G., and Cavieres, J. D. (1998) *J. Biol. Chem. 273*, 14277−14284, 33759−33765]. Native and FITC-modified enzymes have now been photolabeled with TNP-8N_3-[α-^{32}P]ADP and α-chain soluble tryptic peptides separated by reverse-phase HPLC. With native Na,K-ATPase, three labeled peaks lead to the unique sequence α-^{470}-Ile-Val-Glu-Ile-Pro-Phe-Asn-Ser-Thr-Asn-X-Tyr-Gln-Leu-Ser-Ile-His-Lys^{487}, the dropped residue being αLys480. With the FITC enzyme, instead, two independent labeling and purification cycles return the sequence α-^{721}Ala-Asp-Ile-Gly-Val-Ala-Met-Gly-Ile-Ala-Gly-Ser-Asp-Val-Ser-Lys^{736}. These results suggest that Na,K-ATPase also has a low-affinity nucleotide binding region, one that is under distinctive allosteric control by Na^+ and K^+. Moreover, the cation effects seem compatible with a slow, passive Na^+/K^+ carrier behavior of the FITC-modified sodium pump.

The sodium pump or Na,K-ATPase[1] mediates active transport of Na^+ and K^+ across the plasma membrane of animal cells, driven by the hydrolysis of ATP (*1*, *2*). Under physiological conditions, three sodium ions are loaded at high-affinity intracellular sites and delivered to the extracellular medium, where two potassium ions bind to the cation sites and are transported inward (*3*−*5*). Enzyme conformers generically termed E1, capable of intracellular sodium binding, also bind ATP with high affinity [K_D = 0.1−0.2 μM (*6*, *7*)]; there are close interactions between both events, which result in phosphorylation of the enzyme (*8*). Following binding of K^+ to the cation sites, now in their extracellular presentation [E2 (*3*−*5*)], the phosphoenzyme is quickly hydrolyzed while the bound K^+ becomes occluded within the enzyme structure (*9*−*12*). Deocclusion of K^+ toward the intracellular medium is rate-limiting at a few micromolar ATP, but this is greatly accelerated by higher concentrations of ATP or nonphosphorylating ATP analogues [$K_{0.5} \approx$ 0.2−0.5 mM (*9*−*12*)]. Those two ATP affinities, as substrate and as regulator, are reflected in a complex ATP dependence of the Na,K-ATPase activity (*13*); this behavior does not require multiple ATP-binding α-subunits, as is also observed with solubilized protomers consisting of one α-chain and one β-chain (*14*).

† This work was supported by research grants from The Wellcome Trust.

* To whom correspondence should be addressed: Department of Cell Physiology and Pharmacology, Faculty of Medicine and Biological Sciences, University of Leicester, Leicester LE1 9HN, United Kingdom. Telephone and fax: +44 116 2523091. E-mail: jdc7@le.ac.uk.

‡ Transport ATPase Laboratory, Department of Cell Physiology & Pharmacology, Faculty of Medicine and Biological Sciences.

§ Present address: CRUK Institute for Cancer Studies, University of Birmingham, Edgbaston, Birmingham B15 2TT, U.K.

∥ Present address: Department of Biology, Lancaster University, Lancaster LA1 4YW, U.K.

⊥ Protein and Nucleic Acid Laboratory.

Present address: Cambridge Centre for Proteomics, Department of Biochemistry, University of Cambridge, Downing Site, Cambridge CB2 1QW, U.K.

[1] Abbreviations: Na,K-ATPase, Na^+- and K^+-activated adenosine triphosphatase (EC 3.6.1.37); FITC, fluorescein 5′-isothiocyanate; TNP-8N_3-ADP, -ATP, and -AMP, 2′(3′)-*O*-(2,4,6-trinitrophenyl)-8-azidoadenosine 5′-diphosphate, 5′-triphosphate, and 5′-monophosphate, respectively; TNP-ATP, -ADP, and -AMP, 2′(3′)-*O*-(2,4,6-trinitrophenyl)adenosine 5′-triphosphate, 5′-diphosphate, and 5′-monophosphate, respectively; 8N_3-ATP, 8-azidoadenosine 5′-triphosphate; 2N_3-ATP, 2-azidoadenosine 5′-triphosphate; *p*NPP, *p*-nitrophenyl phosphate; PLP, pyridoxal 5′-phosphate; AP_2PL, pyridoxal 5′-diphospho-5′-adenosine; SERCA, sarco(endo)plasmic reticulum Ca^{2+}-ATPase 1A; TES, *N*-tris(hydroxymethyl)methyl-2-aminoethanesulfonic acid; TPCK, *N*-tosyl-L-phenylalanine chloromethyl ketone; RP-HPLC, reverse-phase high-performance liquid chromatography; TFA, trifluoroacetic acid; DIDS, 4,4′-diisothiocyanostilbene 2,2′-disulfonic acid; H_2DIDS, dihydro-4,4′-diisothiocyanostilbene 2,2′-disulfonic acid; FSBA, 5′-(*p*-fluorosulfonyl)benzoyladenosine; ClR-ATP, γ-[4-(*N*-2-chloroethyl-*N*-methylamino)]benzylamide ATP; AMP-PCP, adenosine 5′-(βγ-methylene)triphosphate.

10.1021/bi051927k CCC: $33.50 © 2006 American Chemical Society
Published on Web 02/11/2006

We have been looking into the nature of the two ATP effects and have used FITC to protect the high-affinity site (*15*). FITC inactivates the sodium pump by virtue of its covalent block of high-affinity ATP binding and ATP phosphorylation of the enzyme; it has little effect on backward phosphorylation by P_i or on the ability of the enzyme to hydrolyze synthetic substrates such as *p*NPP in the presence of K^+ (*16*−*18*). Nucleotides have a biphasic effect on this K^+-phosphatase activity; the FITC modification eliminates the high-affinity ATP activation (*19*) but not the low-affinity inhibition by ATP, TNP-ATP, and TNP-ADP (*15*, *19*). This makes FITC a sharp instrument for dissecting E1 from E2 reactions, other affinity labels being less discriminatory (*18*). The inhibitory nucleotide effects offer a convenient means of monitoring low-affinity binding while avoiding the difficulties associated with equilibrium measurements at high ligand concentrations. Because of the higher intrinsic affinity conferred by the trinitrophenyl group, we used TNP-8N_3-ADP to photoinactivate the surviving functions as well as photolabel the FITC-modified Na,K-ATPase (*18*, *20*). We found that Mg^{2+} or high Na^+ concentrations were needed to promote significant photoinactivation and labeling, their effects being countered by K^+. We also observed that much lower TNP-8N_3-ADP concentrations sufficed to photoinactivate the Na,K-ATPase activity of the native enzyme (*18*) or photolabel its α-chain (*20*); in this case, Na^+ did not increase the degree of labeling, yet K^+ still decreased it.

We have now investigated the anchoring sites for TNP-8N_3-[α-^{32}P]ADP on both native and FITC-modified Na,K-ATPase and have examined the photoinactivation requirements more closely. We find that the probe becomes covalently attached to αLys480 following photolabeling of the native enzyme with TNP-8N_3-[α-^{32}P]ADP; K^+ and Na^+ modulate the process with very high affinities. In the structurally similar Ca^{2+} pump of the sarcoplasmic reticulum (SERCA), the homologous residue (*21*, *22*) is *s*Lys492; in SERCA's crystal structure (*23*), this is found at the entrance of a pocket in the "nucleotide" (N) domain. With the FITC-modified enzyme, instead, TNP-8N_3-[α-^{32}P]ADP labels the peptide α-^{721}ADIGVA...K^{736}. If the homology described above is applied, this sequence should map to the "phosphorylation" (P) domain of Na,K-ATPase, as part of a putative Rossman fold.

MATERIALS AND METHODS

Enzyme Purification. Na,K-ATPase was purified from pig kidneys by the zonal rotor method of Jørgensen (*24*). The Na,K-ATPase activity at 37 °C ranged from 20 to 35 μmol min^{-1} mg^{-1}.

Na,K-ATPase Assays. During and before UV irradiation, the Na,K-ATPase activity was measured in triplicate at 37 °C with a coupled-enzyme spectrophotometric assay (*18*), in 1 mL of a medium containing 140 mM NaCl, 15 mM KCl, 25 mM histidine (pH 7.4), 2 mM ATP, 3 mM $MgCl_2$, 1 mM phosphoenolpyruvate, 0.15 mM NADH, 15 units of pyruvate kinase, and 15 units of lactate dehydrogenase. The solutions were pre-equilibrated to temperature, and the cuvettes were continually stirred in the thermostated six-cell positioner of a U-3310 Hitachi spectrophotometer. Na,K-ATPase activities were obtained from the linear segment of the NADH absorbance decrease at 338 nm (6−10 data points over 5 min), fitted by least-squares regression.

K^+-Phosphatase Assays. The assay (*15*) was carried out with 20 μL samples of enzyme suspensions in 340 μL of a medium consisting of 20 mM KCl, 6 mM $MgCl_2$, 20 mM Tris-HCl (pH 7.5), 1 mM EDTA, and 10 mM *p*NPP (diTris salt). Reactions of six 50 μL samples were stopped in 0.3 mL of 0.1 M NaOH every 30 s, and the released *p*-nitrophenol was read at 410 nm against a calibration curve. Enzymatic rates and their errors were calculated from the slopes of linear time courses.

FITC Treatment. This was done largely as described previously (*20*). Briefly, the enzyme (at 1 mg/mL) was incubated at 20 °C for 30 min and in the dark with 50 μM FITC in the presence of 100 mM NaCl, 50 mM Tris-HCl (pH 9.2), and 5 mM EDTA. After being washed by ultracentrifugation, the enzyme was resuspended in 20 mM Tris-HCl (pH 7.5) and 1 mM EDTA and assayed for protein and Na,K-ATPase activity, together with parallel FITC-free controls.

TNP-8N_3-ADP, TNP-8N_3-[α-^{32}P]ADP, and TNP-ATP Syntheses. Addition of the TNP group was carried out as described previously (*25*), and the products were purified by reverse-phase HPLC (*18*). 8N_3-[α-^{32}P]ATP was either purchased or synthesized from [α-^{32}P]ATP (*20*), and 8N_3-[α-^{32}P]ADP was prepared by hydrolyzing 8N_3-[α-^{32}P]ATP with Na,K-ATPase (*20*). All products were checked for purity by analytical HPLC and characterized via their absorption spectra and acid-labile phosphate stoichiometries (*18*, *26*).

TNP-8N_3-ADP Photoinactivation and Photolabeling. The UV irradiation was carried out using a Flowgen VL-6MC UV lamp (6 W output) set at 312 nm, and from a distance of 50 cm inside an opaque box at constant temperature and humidity. The samples were contained in a 24-well plate filled to a depth of 2−3 mm and sitting on an aluminum plate kept at 20 °C. The exposure was interrupted to withdraw 10 μL samples (1−2 μg of protein) for Na,K-ATPase activity determinations. For kinetic experiments, the enzyme (final concentration of 0.2 mg/mL, nominally 1.3 μM in high-affinity nucleotide sites) was usually photoinactivated in 400 μL of a basic medium containing 50 mM Tris-HCl (pH 7.5) and 1 mM EDTA ("TE50-1"). This was done at variable irradiation times and TNP-8N_3-ADP concentrations, or for 10 min at 2 μM probe; other additions are specified in the figure legends. For radioactive labeling, 5−10 mg of native or FITC-modified Na,K-ATPase was spun down in a Beckman TL-100 ultracentrifuge (15 min at 356000*g*) and resuspended at 0.15−0.20 mg/mL in 12 mL of a solution containing 150 mM NaCl, 20 mM Tris-HCl (pH 7.5 at room temperature), 1 mM EDTA, and 0.1−0.5 MBq of TNP-8N_3-[α-^{32}P]ADP. The latter was at a concentration of 5 μM with the native enzyme and 15−30 μM with the FITC-labeled enzyme (*20*). Having sampled for enzyme activity determinations before and after a 30 min irradiation, we spun down the remaining suspension as described above and washed with probe-free NaCl/Tris/EDTA solution, as above; the final pellet was solubilized with 10% SDS, 25 mM imidazole (pH 7.4), and 1 mM EDTA.

Size-Exclusion Chromatography of Solubilized Na,K-ATPase Subunits. The labeled, SDS-treated pellet described above was spun out in the benchtop ultracentrifuge, and the supernatant was loaded onto a Superdex-200 column (Am-

ersham Biotech, 16 mm × 600 mm) pre-equilibrated for 24 h with a buffer containing 20 mM TES (pH 7.0), 1 mM EDTA, and 0.5% SDS. The column was eluted with the solution described above, delivered isocratically with a Pharmacia/LKB 2248 HPLC pump at 0.5 mL/min. The effluent was monitored at 230 nm with a Pharmacia/LKB VWM2141 detector and collected as 90 × 2 min fractions.

Trypsin Digestion. The pooled fractions corresponding to the α-chain peak (ca. 30 wt % of total protein, Figure 6) were kept overnight at −20 °C after addition of 2 volumes of chilled acetone. Following centrifugation at 3000*g* for 30 min, the pellet was allowed to dry, taken up in 0.3−0.4 mL of 8 M urea, and incubated for 1 h at 37 °C. The suspension was diluted 4-fold with 20 mM Tris-HCl (pH 8.0) and 1 mM EDTA containing sequencing-grade TPCK-treated trypsin at a 1:10 trypsin:α-chain gram ratio, incubated for 3 h at 37 °C, and centrifuged for 15 min at 435000*g*.

Peptide Purification. In the case of the native enzyme, the supernatant described above was loaded onto a Vydac C_4 reverse-phase column (5 μm, 4.6 mm × 250 mm with a 3 mm × 4 mm guard) equilibrated with 20 mM Na^+ phosphate (pH 6.0) (*solvent A*). The column was developed with a 0 to 100% gradient of methanol (*solvent B*) over 90 min, at 1 mL/min, using a titanium system including two Pharmacia/LKB 2248 HPLC pumps, an LCC2252 controller, and a Pharmacia high-pressure mixer. The absorbance of the eluate was followed at 230 nm, and 1 min fractions were collected and 20 μL aliquots assessed for ^{32}P. The fractions containing the main radioactivity peak were pooled, chilled, dried under vacuum, and subjected to a second reverse-phase HPLC on a C_{18} column (Vydac, 5 μm, 4.6 mm × 250 mm with a guard) with 0.1% (v/v) TFA as solvent A and methanol as solvent B. The sample (in 10% B) was injected into the pre-equilibrated column and developed over 90 min with the following gradient: 10% B at 0 min, 62.5% B at 60 min, and 100% B at 90 min (at 1 mL/min); 1 min fractions were collected and aliquots assessed. With the FITC-modified enzyme, better separations were achieved by starting with the C_{18} column. Solvent A was 20 mM Na^+ phosphate (pH 6.5), and solvent B was methanol. Initially, the gradient was from 10% B at 0 min to 80% B at 110 min to 100% B at 111 min but was later changed to begin at 0% B. Fractions containing radioactive peaks were dried under vacuum, redissolved in 0.1% TFA, and rechromatographed on a C_4 column with 0.1% (v/v) TFA as solvent A, methanol as solvent B, and the following gradient: 10% B at 0 min, 80% B at 110 min, and 100% B at 111 min.

Peptide Sequencing. Purified peptides were covalently attached to Sequelon amino aryl disks and N-terminally sequenced using an Applied Biosystems 476 protein sequencer (Applied Biosystems, Warrington, U.K.).

Protein Determinations. The amount of protein was determined with a modified bicinchoninic acid assay, using bovine serum albumin as the standard (*14*, *27*).

SDS−PAGE. This was carried out in 7.5% T minigels prepared according to the method of Laemmli (*28*) or in Tricine minigels (*29*).

Data Handling. When native enzyme inactivation was observed against time (e.g., Figure 1), the natural logarithm of the remaining fraction was plotted against time. The slopes of the least-squares straight lines returned the negative value of the inactivation rate constant (k_x). When the inactivation was done for a fixed period t, k_x was calculated as $\ln(A_0/A)/t$, from triplicate estimates of Na,K-ATPase or K^+-phosphatase activity at time zero (A_0) and time t (A), and the errors were compounded. For TNP-$8N_3$-ADP photoinactivation of the native enzyme, $t = 10$ min; for the FITC-labeled enzyme, $t = 30$ min. Nonlinear regressions were done with Sigmaplot 2002 version 8 (SPSS Inc., Chicago, IL).

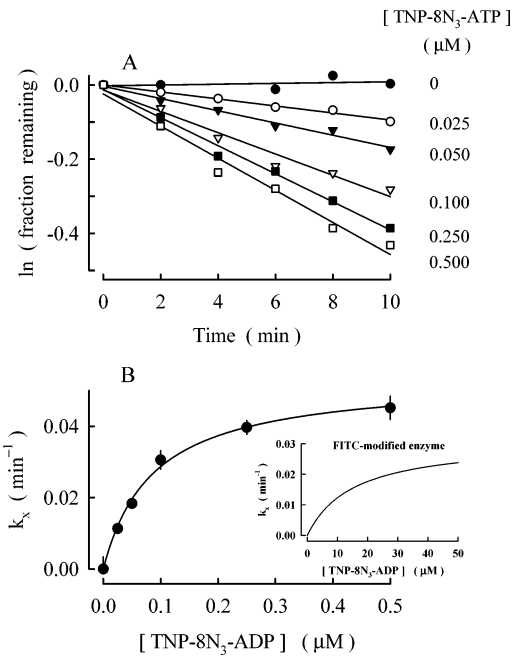

FIGURE 1: Time courses and TNP-$8N_3$-ADP concentration dependence of the photoinactivation of native Na,K-ATPase. The purified enzyme at 0.1 mg/mL was mixed with TNP-$8N_3$-ADP dilutions in TE50-1 medium (see Materials and Methods). The suspensions were irradiated at 312 nm, and the Na,K-ATPase activity was measured. (A) Photoinactivation time courses, at the TNP-$8N_3$-ADP concentrations shown. The natural logarithm of the fractional Na,K-ATPase activity remaining is plotted against the irradiation time; the fitted slope returns the inactivation rate constant (k_x). (B) Net k_x plotted against the TNP-$8N_3$-ADP concentration. The line represents the equation $y = ax/(b + x)$, fitted with an a [or $k_{x(max)}$] of 0.054 ± 0.002 min^{-1} and a b [or $K_{D(TNP-8N_3-ADP)}$] of 0.087 ± 0.009 μM. Vertical lines show the compounded standard errors. The inset shows the photoinactivation of the K^+-phosphatase activity of the FITC-modified sodium pump (remaining Na,K-ATPase activity of ≈2%). Hyperbola as above, but with a net $k_{x(max)}$ of 0.031 min^{-1} and a $K_{D(TNP-8N_3-ADP)}$ of 15 μM (parameters from ref *18*).

Source of Materials. ATP, disodium salt (special quality), was from Roche Molecular Biochemicals and was used for ATPase assays and for $8N_3$-[α-^{32}P]ATP and TNP-ATP syntheses (TNP-ATP was also purchased from Molecular Probes). [α-^{32}P]ATP was bought from NEN Life Science Products, and alternatively, $8N_3$-[α-^{32}P]ATP was obtained from ICN Pharmaceuticals (Irvine, CA) or Affinity Labeling Technologies (Lexington, KY). *p*NPP (di-Tris salt) was from Sigma London. Specpure NaCl and KCl were from Johnson Matthey (Alfa Aesar, Karlsruhe, Germany). TPCK-treated bovine trypsin (sequencing-grade) was purchased from Worthington Biochemical Corp. (Lakewood, NJ), and Sequelon amino aryl disks were from Applied Biosystems. Redistilled TFA was from Aldrich (Gillingham, U.K.), and methanol (HPLC quality) and urea were from Fisher Scientific (Loughborough, U.K.). Vydac RP-HPLC columns were purchased from Hichrom (Reading, U.K.). All other reagents were of the maximal available purity.

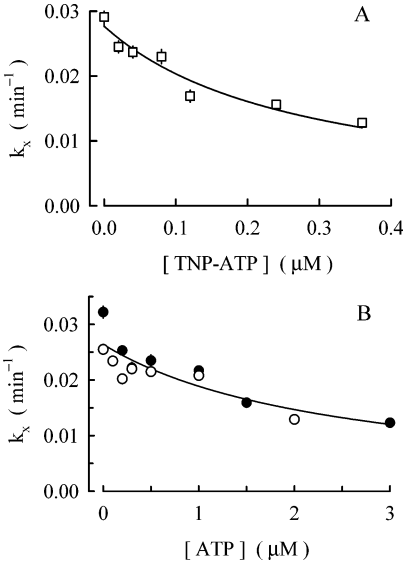

FIGURE 2: TNP-ATP and ATP protect native Na,K-ATPase from TNP-8N$_3$-ADP photoinactivation. The enzyme was irradiated (see Figure 1) for 10 min with or without 0.2 μM TNP-8N$_3$-ADP, and inactivation rate constants were calculated from triplicate ATPase determinations and by reference to zero-time values. (A) Protection by TNP-ATP. The data have been fitted to the decaying hyperbola $y = ab/(b + x)$, where $a = 0.028 \pm 0.001$ min^{-1} and b [or $K_{0.5(TNP-ATP)}$] $= 0.28 \pm 0.05$ μM. (B) Protection by ATP, in two separate experiments. The combined data were fitted as described above, with a $K_{0.5(ATP)}$ of 2.5 ± 0.6 μM.

RESULTS

Effect of Ligands on TNP-8N$_3$-ADP Photoinactivation of Native Na,K-ATPase. Figure 1A shows that the inactivation proceeds as a monoexponential decay for at least 10 min. When plotted against the TNP-8N$_3$-ADP concentration, k_x increases in a saturable fashion (Figure 1B), and the good hyperbolic fit is good evidence that formation of an equilibrium TNP-8N$_3$-ADP·enzyme complex precedes covalent attachment (*30*). The result shows a high-affinity dependence on the TNP-8N$_3$-ADP concentration, and this experiment returns a $K_{D(TNP-8N_3-ADP)}$ of 0.09 ± 0.01 μM (mean $\pm$ the standard error). Two other experiments gave similar results; when all three are pooled, $K_{D(TNP-8N_3-ADP)} = 0.11 \pm 0.02$ μM.

ATP and TNP-ADP prevent photolabeling of the native sodium pump by TNP-8N$_3$-[α-^{32}P]ADP (*20*), and TNP-ADP prevents the photoinactivation of its Na,K-ATPase activity (*18*); Figure 2 shows the concentration dependence of the ATP and TNP-ATP protective effects at 0.2 μM TNP-8N$_3$-ADP. Assuming direct competition between TNP-ATP and TNP-8N$_3$-ADP and using a $K_{D(TNP-8N_3-ADP)}$ of 0.11 μM (above) and a $K_{0.5(TNP-ATP)}$ of 0.28 μM (Figure 2A), we calculate an inhibition constant $K_{i(TNP-ATP)}$ of 0.28/(0.20/0.11 + 1) = 0.10 μM; a similar calculation for ATP (Figure 2B) gives a $K_{i(ATP)}$ of 0.89 μM. Therefore, our estimates for the TNP-8N$_3$-ADP and TNP-ATP dissociation constants are essentially the same and 8−9 times lower than that for ATP; they are comparable or lower than binding constants obtained from TNP-[^{3}H]ATP binding or fluorimetric titrations (*31*). All of these values are consistent with binding at a high-affinity nucleotide site on Na,K-ATPase (*6*, *7*). The inset in Figure 1B shows, for comparison, the fitted concentration dependence of the TNP-8N$_3$-ADP photoinactivation of the K$^+$-phosphatase activity of the FITC-modified enzyme (replotted from ref *18*), where $K_{D(TNP-8N_3-ADP)}$ equaled 15 μM.

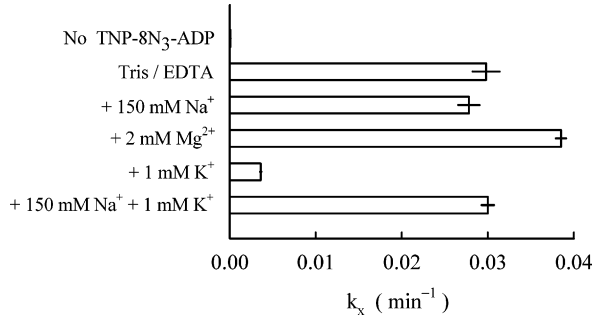

FIGURE 3: Effects of Na$^+$, K$^+$, and Mg^{2+} on TNP-8N$_3$-ADP photoinactivation of native Na,K-ATPase. Enzyme samples in TE50-1 were irradiated for 10 min in the absence (top bar) or presence (other bars) of 0.2 μM TNP-8N$_3$-ADP, without (top two bars) or with Na$^+$, K$^+$, or Mg^{2+} added to the TE50-1 medium. Rate constants were calculated as described in the legend of Figure 2, from triplicate irradiated and zero-time samples. Horizontal lines represent compounded standard errors.

The effects of Na$^+$, K$^+$, and Mg^{2+} on the inactivation rate constant are shown in Figure 3. With 1 mM EDTA in the medium, the addition of 2 mM Mg^{2+} caused an only modest increase in k_x, and this agrees with the apparent lack of an effect of Mg^{2+} on the photolabeling of native Na,K-ATPase (*20*). This seems different from the Mg^{2+} requirement for 8N$_3$-ATP photoinactivation (*32*) or TNP-8N$_3$-ADP photolabeling of FITC-modified Na,K-ATPase or photoinactivation of its K$^+$-phosphatase activity (*18*, *20*). In this case, the small effect probably means that the TNP-8N$_3$-ADP·Mg^{2+} complex is a marginally better ligand than free TNP-8N$_3$-ADP (*20*) rather than Mg^{2+} acting by promoting an E1 form of the enzyme (*33*). That the native Na,K-ATPase spontaneously adopts an E1 conformation under our conditions is clearly shown by the lack of an effect of 150 mM NaCl (Figure 3), and the fact that 1 mM KCl decreases k_x to a low value. These Na$^+$ and K$^+$ results have their counterpart on the photolabeling of the native enzyme with TNP-8N$_3$-[α-^{32}P]ADP, where Na$^+$ had no effect and K$^+$ decreased the incorporation level (Figure 1 of ref *20*). Figure 3 also shows that Na$^+$ cancels the K$^+$ effect. Both individual and combined Na$^+$ and K$^+$ results thus mirror the effects of these cations on equilibrium ATP binding at a high-affinity site on Na,K-ATPase (*6*, *7*). Despite the dispersion in the data, Figure 4A shows that K$^+$ is effective at very low concentrations; we limited curve fitting to a two-parameter function, and taking the results at face value and considering all three experiments, we found $K_K' = 12 \pm 4$ μM. The Na$^+$ reversal of the effect of 30 μM K$^+$ is shown in Figure 4B, where the hyperbolic fitting returns a K_{Na}' of 0.58 ± 0.08 mM. The insets in Figure 4 show the cation effects on the TNP-8N$_3$-ADP photoinactivation of the K$^+$-phosphatase activity of the FITC-labeled enzyme (replotted from ref *20*), which occurred with much higher $K_{0.5}$ values.

Nature of the Low-Affinity Na$^+$ Effect on the TNP-8N$_3$-ADP Photoinactivation of the FITC-Modified Na,K-ATPase. We looked at the TNP-8N$_3$-ADP concentration dependence of the inactivation, in the presence of both 200 and 10 mM Na$^+$ (instead of nominally zero Na$^+$, to exclude possible effects of Na$^+$ or K$^+$ contamination). Figure 5, where hyperbolae have been fitted to the pooled sets of data, shows

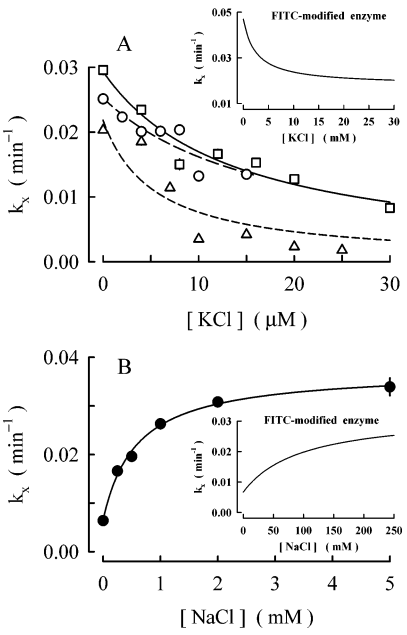

FIGURE 4: Protection by K^+ and its reversal by Na^+. Native Na,K-ATPase was photoinactivated as described in the legend of Figure 2. (A) Three experiments showing the effect of KCl (Specpure) added during irradiation. The decaying hyperbolae have been fitted as in Figure 2, with an apparent affinity K_K' of 14 ± 2 (−□−), 18 ± 5 (−○−), and 5 ± 2 μM (-△-). The inset shows the effect of K^+ on k_x of K^+-phosphatase activity of FITC-modified Na,K-ATPase. The line was drawn with a $K_{0.5(K)}$ of 2.5 mM, according to ref *20*. (B) Effect of increasing the concentration of NaCl (Specpure) on the TNP-8N_3-ADP inactivation in the presence of 30 μM K^+. The hyperbola has been fitted with a K_{Na}' of 0.58 ± 0.08 mM. Standard errors are shown as vertical bars or are comprised within the symbols. The inset shows the effect of Na^+ on the TNP-8N_3-ADP inactivation of the FITC-modified sodium pump (in the absence of K^+), drawn with a $K_{0.5(Na)}$ of 97 mM (*20*).

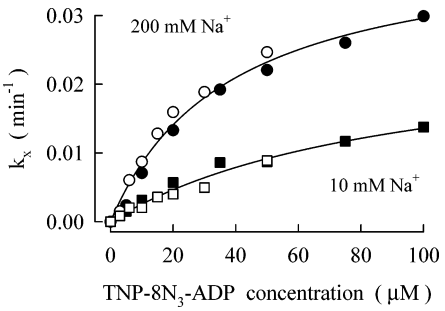

FIGURE 5: Regulatory effect of Na^+ on the TNP-8N_3-ADP photoinactivation of FITC-modified Na,K-ATPase. Two experiments, up to 50 μM (empty symbols) and 100 μM probe (filled symbols), using the same stock TNP-8N_3-ADP solution and the same batch of FITC-modified sodium pump (0.4% Na,K-ATPase activity left). The K^+-phosphatase activity was photoinactivated for 30 min in 20 mM Tris-HCl (pH 7.5), 1 mM EDTA, and 10 mM NaCl (squares) or 200 mM NaCl (circles). Inactivation rate constants were calculated as described in the legend of Figure 2, from triplicate "initial" and "final" K^+-phosphatase activity determinations. Hyperbolae were fitted to the combined data as in Figure 1B, with $k_{x(max)}$ values of 0.026 ± 0.004 min^{-1} (10 mM Na^+) and 0.041 ± 0.003 min^{-1} (200 mM Na^+) and $K_{D(TNP-8N_3-ADP)}$ values of 93 ± 21 μM (10 mM Na^+) and 37 ± 5 μM (200 mM Na^+).

the results of two experiments. The parameters indicate that a high Na^+ concentration has mixed effects, increasing the TNP-8N_3-ADP binding affinity 2.5 times and the reactivity toward the 8-nitrene radical by nearly 60%. Considering our earlier results (*18*, *20*), it is now evident that the low-affinity

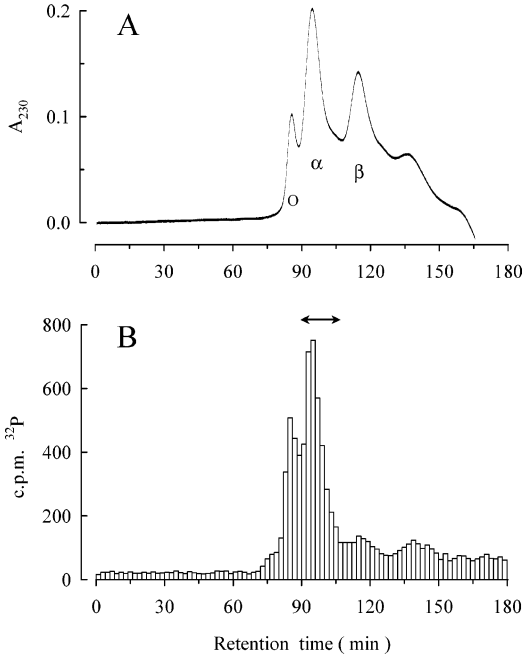

FIGURE 6: Size-exclusion chromatography of solubilized native Na,K-ATPase labeled with TNP-8N_3-[α-^{32}P]ADP. Native Na,K-ATPase (5 mg) was photolabeled for 30 min with 5 μM TNP-8N_3-[α-^{32}P]ADP (see Materials and Methods); 33% of the Na,K-ATPase activity remained. The labeled enzyme was solubilized with a buffer containing 10% SDS, and the high-speed supernatant was loaded onto a Superdex-200 column (16 mm × 600 mm) pre-equilibrated for 24 h with 20 mM TES (pH 7.0), 1 mM EDTA, and 0.5% SDS. The column was eluted with the solution described above at 0.5 mL/min, and 90 × 2 min fractions were collected. (A) Absorbance of the effluent at 230 nm. Aliquots of the fractions were run in SDS−PAGE Laemmli gels (not shown). The first peak (O, maximum of 85.5 min) consisted of a mixture of various stable oligomers of α- and β-subunits; the second (α, maximum of 94.5 min) contained the α-chain plus some aggregates, and the third (β, maximum of 114.5 min) showed the diffuse β-subunit and a few faint, fast-migrating bands, presumably proteolytic products. (B) Radioactivity in the fractions. Fractions 45−53 (90−106 min, double-headed arrow) were pooled.

Na^+ requirement is not absolute, for photoinactivation of the FITC-labeled enzyme. At 10 mM Na^+, TNP-8N_3-ADP can still bind at its site even if with a lower affinity, and the photoinactivation persists, although at a slower rate.

Purification and Sequencing of Photolabeled Peptides. Autoradiograms of SDS−PAGE gels of native Na,K-ATPase photolabeled with TNP-8N_3-[α-^{32}P]ADP had shown that most of the label migrated with the α-chain (Figure 1 of ref *20*). Nevertheless, we isolated the labeled α-subunit by size-exclusion chromatography, to facilitate the purification of the tryptic peptides and remove loosely bound probe. Figure 6A shows the elution after SDS solubilization, where the α-subunit appears to be reasonably well separated from the β-chain. Figure 6B shows that most of the radioactivity is associated with the α-chain and oligomer peaks and that little label elutes under the β-chain peak, as expected (*20*); the remaining radioactivity appears on smaller micelles, probably associated with proteolytic products, or as a free probe at long times. The pooled, labeled α-chain was precipitated with acetone and the pellet solubilized with 8 M urea. Following a 4-fold dilution, the material was digested with TPCK-treated trypsin, and judging from the results of tricine SDS−PAGE (*29*), all α-chain or large peptides had disappeared after a 3 h digestion at 37 °C (not shown).

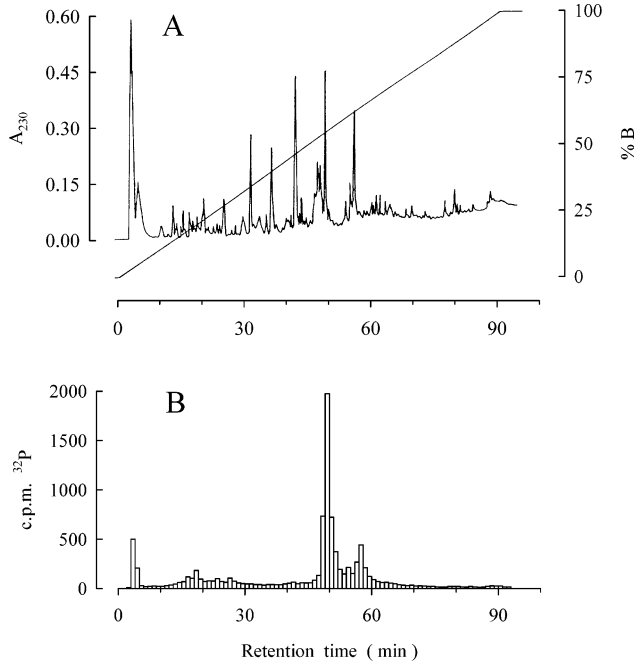

FIGURE 7: Separation of soluble tryptic peptides of TNP-8N$_3$-[α-^{32}P]ADP-labeled native Na,K-ATPase via C$_4$ reverse-phase HPLC. The pooled α-chain (as in Figure 6) was precipitated, redissolved, and trypsinized (see Materials and Methods). Aliquots of the 435000*g* supernatant were loaded onto a Vydac C$_4$ column equilibrated with 20 mM Na^+ phosphate at pH 6.0 (solvent A), and the column was developed with a 0 to 100% gradient of methanol (solvent B) at a rate of 1 mL/min. One minute fractions were collected. (A) The trace shows the absorbance of the eluate at 230 nm (left axis) and the segment line the linear solvent gradient (right axis). (B) A 20 μL sample of each fraction was assessed for ^{32}P.

The soluble tryptic peptides of the TNP-8N$_3$-[α-^{32}P]ADP-labeled, native α-subunit were subjected to reverse-phase separation on a C$_4$ column, shown in Figure 7. The main radioactive peak (fractions 49−51) was rechromatographed on a C$_{18}$ column (Figure 8). Aliquots from both C$_{18}$ radioactive peaks (Figure 8B, fractions 47 and 52, around 3000 cpm or 70 pmol each) were taken for automated Edman degradation. Figure 9 shows the results for both fractions and also for a second full labeling and sequencing round (C$_4$ peak centered around fraction 75, re-emerging as fractions 72 and 73 on C$_{18}$ rechromatography). All fractions returned essentially the same sequence. In fraction 47 and fractions 72 and 73, the signal became too weak to call the residues unambiguously beyond cycles 14 and 16, respectively; this also happened with cycle 15 of fraction 52, but in this case, the sequence resumed, to terminate abruptly after cycle 18. The sequence in Figure 9 corresponds to the α-chain fragment ^{470}Ile-Val-Glu-Ile-Pro-Phe-Asn-Ser-Thr-Asn-X-Tyr-Gln-Leu-Ser-Ile-His-Lys^{487} of pig kidney Na,K-ATPase (*34*), where the common dropped residue is αLys480. This should be the point of covalent attachment, as the eluted probe−lysine adduct would not be recognized by the amino acid analyzer. The TNP-8N$_3$-[α-^{32}P]ADP anchoring residue on native Na,K-ATPase is, therefore, the same as for 8N$_3$-ATP (*35*), AP$_2$PL, or PLP (*36*) and homologous to the attachment point for TNP-8N$_3$-ATP and TNP-8N$_3$-AMP in rabbit skeletal muscle SERCA [*s*Lys492 (*37*)].

To photolabel the FITC-modified Na,K-ATPase, the TNP-8N$_3$-[α-^{32}P]ADP concentration was increased at least 5-fold

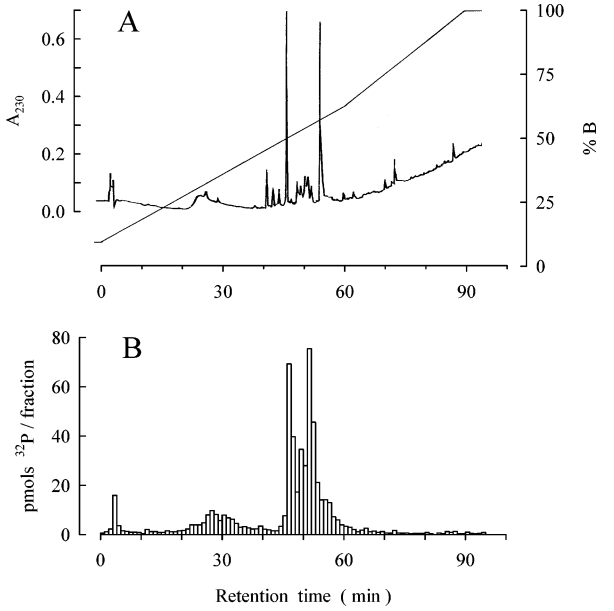

FIGURE 8: Rechromatography on a C$_{18}$ column. Fractions 49−51 from the C$_4$ chromatography (Figure 7) were pooled and dried under vacuum, dissolved in 10% B (solvent A being 0.1% TFA and solvent B being methanol), and loaded onto a Vydac C$_{18}$ reverse-phase column pre-equilibrated with 10% B. (A) The segment line (right axis) shows the 10 to 100% B gradient, at a flow rate of 1 mL/min; the trace represents the absorbance at 230 nm (left axis). (B) ^{32}P radioactivity in 100 μL samples of 1 min fractions.

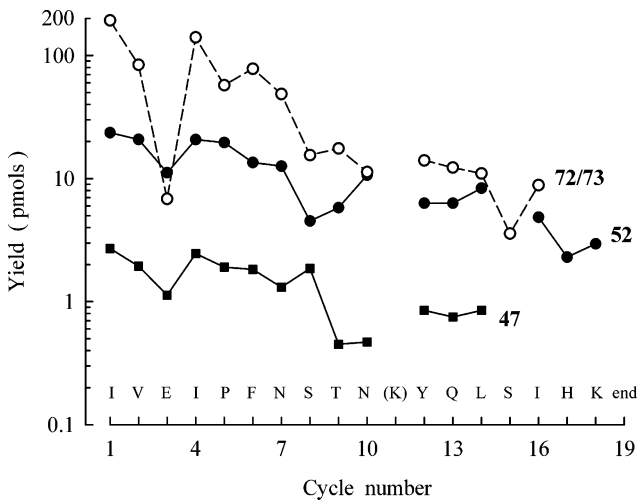

FIGURE 9: Amino acid sequence of the TNP-8N$_3$-[α-^{32}P]ADP-binding peptide in native Na,K-ATPase. The two main peaks in Figure 8B (fractions 47 and 52) were sequenced by automated Edman degradation (solid symbols and lines): (■) fraction 47 and (●) fraction 52 (the latter sharply terminated after cycle 18). In addition, the result of another mapping experiment is also shown, leading to a C$_4$ peak centered on fraction 75, re-emerging as fractions 72 and 73 from the C$_{18}$ column (○). All peptides returned sections from the same sequence, as shown; cycle 11 did not lead to positive identification in the phenylthiohydantoin chromatogram. The sequence matches the ^{470}IVEI...K^{487} segment of the α-chain of pig kidney Na,K-ATPase (*33*), where the common missing residue is αLys480.

and 100 mM Na^+ was added (*20*). When the soluble tryptic peptides were analyzed with the C$_4$ column (not shown), the prominent 50 or 75 min radioactive peaks were virtually absent, despite the higher TNP-8N$_3$-[α-^{32}P]ADP concentration. This was to be expected, as FITC is quite effective at blocking access to the high-affinity nucleotide site (*16*, *18*).

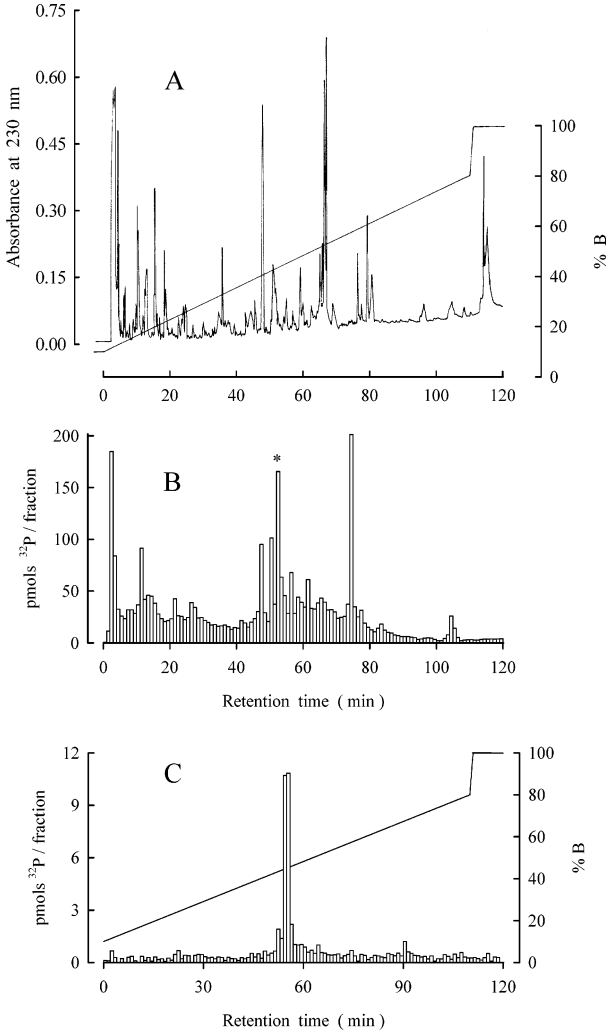

FIGURE 10: Separation of soluble tryptic α-chain peptides of the FITC-modified sodium pump after labeling with TNP-8N_3-[α-^{32}P]-ADP. The FITC-modified enzyme (8.7 mg, Na,K-ATPase activity of <1%, K^+-phosphatase activity of >90%) was incubated with 15 μM TNP-8N_3-[α-^{32}P]ADP for 30 min in a 100 mM Na^+ medium; its K^+-phosphatase activity decreased to 75%. The α-subunit was separated as shown in Figure 6, and trypsinized overnight. (A) The dried soluble peptides were dissolved in 10% B (solvent A being 20 mM sodium phosphate at pH 6.5 and solvent B being methanol) and separated on a C_{18} reverse-phase HPLC column at 1 mL/min with the gradient shown on the right axis. The trace shows the absorbance at 230 nm (left axis). (B) Aliquots of the fractions (50 μL) were assessed for ^{32}P. (C) Fraction 53 in the separation above (asterisk in panel B) was dried, dissolved in 10% B (solvent A being 0.1% TFA and solvent B being methanol), and rechromatographed on a C_4 column with the gradient shown on the right axis, and 1 min fractions were collected. Samples (100 μL) were assessed for ^{32}P.

As the various radioactive peaks were not well resolved, we started with a C_{18} column instead, and the results are shown in panels A and B of Figure 10. All main radioactive C_{18} peaks (Figure 10B) were rechromatographed on a C_4 column: fractions 12 and 75 led to well-defined C_4 peaks (at 23 and 91 min, respectively), without associated sequences, and must represent TNP-8N_3-[α-^{32}P]ADP derivatives released from the protein during the trypsin digestion and latter stages. Fractions 48, 51, 57, and 62 gave either very small radioactive peaks or a noisy elution and were not amenable to further analysis. Fraction 53, however (asterisk in Figure 10B), led to a maximum at 55−56 min

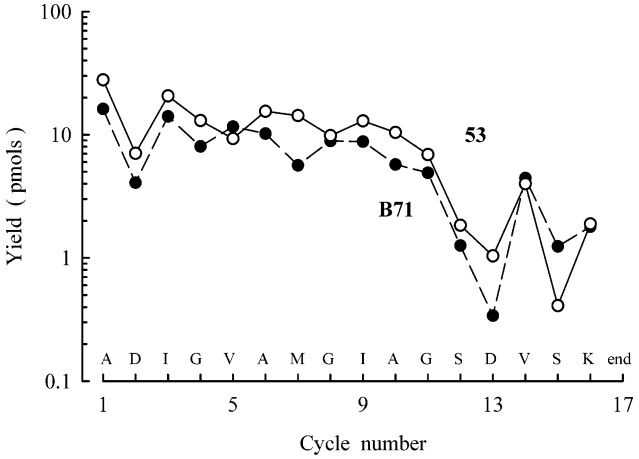

FIGURE 11: Amino acid sequence of the TNP-8N_3-[α-^{32}P]ADP-binding peptide of FITC-modified Na,K-ATPase. The peak consisting of fractions 55 and 56 after C_4 chromatography (Figure 10C) of freezed-dried fraction 53 of Figure 10B (asterisk) was subjected to automated Edman degradation (—○—). The sequence, shown above the abscissa, maps to the ^{721}ADIGVA...K^{736} tryptic fragment of the α-chain of Na,K-ATPase (*33*). In a second labeling and mapping experiment (4 mg of FITC-treated enzyme, Na,K-ATPase activity of 0.4%), a C_{18} RP-HPLC gradient similar to that in Figure 10A was used, now starting at 0% B; three major peaks were obtained, centered at 32−33 (A), 69−70 (B), and 89−90 min (C). Following C_4 rechromatography, B was resolved with a prominent radioactive maximum in fraction 71. The filled symbols and dashed line show the Edman yield, the sequence being identical to that for peptide 53.

(Figure 10C) that returned a unique sequence matching the α-chain fragment ^{721}Ala-Asp-Ile-Gly-Val-Ala-Met-Gly-Ile-Ala-Gly-Ser-Asp-Val-Ser-Lys^{736} [Figure 11 (○)]. This is comprised within the C-terminal 57 kDa α-chain fragment, which bears the TNP-8N_3-[α-^{32}P]ADP label in the FITC-modified enzyme (*20*). Although the downstream aspartate and serine residues were returned in low yields (Figure 11), none of the sequencing cycles was convincingly blank, presumably because the Edman degradations (*38*) progressively removed the radioactive probe from the membrane-attached peptide. Scintillation counting of the material cleaved during each cycle (not shown) returned very low levels of radioactivity, with most ^{32}P probe found binding to the processed Sequelon disk; this has been found with the 2N_3-ATP-labeled peptide (*39*).

FITC-modified Na,K-ATPase was also photolabeled in the presence and absence of 200 μM vanadate, as this transition-state analogue interferes with both TNP-8N_3-[α-^{32}P]ADP photoinactivation and labeling of the FITC-modified Na,K-ATPase (*20*). The tryptic peptides were analyzed on a C_{18} column with a similar gradient, but now starting at 0% B. The radioactive profiles (not shown) consisted of three clusters centered at 25 (A), 70 (B), and 90 min (C). As only B was differentially depressed by the presence of vanadate, A and C probably represent nonspecific label incorporation, forms of free probe released from the labeled peptides, or both. In a preparative photolabeling and purification round, the peak C_{18} fractions for zones B (69−70 min) and C (89−90 min) were rerun on a C_4 column; well-defined peaks were obtained, and as expected, that arising from zone C returned no sequence. The material from zone B, which emerged at 71 min from the C_4 column, led to the result shown in

Figure 11 (●), i.e., to a sequence identical to that found earlier for C_{18} peptide 53.

The FITC-Anchoring Peptide. We sought to verify the attachment point of the fluoresceinyl group on the FITC-modified enzyme under our own experimental conditions. In the C_{18} separation of Figure 10A, most if not all FITC fluorescence emerged at 67 min, in a fraction that strongly absorbed at 500 nm (0.24 AU, ≥3 nmol of fluorescein ≈ nanomoles of α-chain loaded). The same occurred in another full labeling and separation round, and both 67 min fractions were pooled and rerun on a C_4 column. A small spike in A_{500} emerged at 65 min, with no associated radioactivity (not shown). Edman sequencing returned the α-subunit fragment ^{496}His-Leu-Leu-Val-Met-X-Gly-Ala-Pro-Glu-Arg^{506}, where the dropped residue matches αLys501. Amino acid analyzer runs of fluoresceinyllysine standards confirmed that the residue cleaved during the sixth sequencing cycle was the derivatized lysine. αLys501 is the main FITC-anchoring point on Na,K-ATPase (*40*).

DISCUSSION

The rate of photoinactivation of native Na,K-ATPase increases hyperbolically with the TNP-8N_3-ADP concentration, with a K_D of 0.11 μM (Figure 1). The protective effect of low concentrations of ATP and TNP-ATP (Figure 2) and the effects of K^+ and Na^+ (Figures 3 and 4) confirm that TNP-8N_3-ADP photoinactivates following binding within a high-affinity nucleotide binding pocket (*6*, *7*). The covalent TNP-8N_3-ADP anchoring point on the native enzyme, αLys480 (Figure 9), is the same as for 8N_3-ATP (*35*). This residue is homologous to *s*Lys492, targeted in SERCA by TNP-8N_3-ATP and TNP-8N_3-AMP (*37*), and found at the entrance of the high-affinity ATP pocket of the N-domain (*23*, *41*, *42*). The good agreement seems to endorse TNP-8N_3-ADP as a reliable ligand for ATP sites in Na,K-ATPase.

SERCA's anchoring point for FITC is *s*Lys515 (*43*), homologous to αLys501 (*40*). In the SERCA structure (*23*), the N-domain nucleotide pocket is delimited by *s*Lys515 at the deep end and *s*Lys492 at the opening. A similar arrangement in the sodium pump might explain why FITC blocks all reactions requiring high-affinity ATP binding, including ATP hydrolysis. The block is likely to be irreversible and comprehensive, as large increases in the ATP concentration fail to restore any part of the lost Na,K-ATPase activity and, also, because of reasons discussed below, in Cation Effects, and elsewhere (*18*). On the other hand, E2 reactions such as P_i phosphorylation and *p*NPP hydrolysis are spared (*16*, *18*); i.e., the latter do not seem to require the N-domain pocket. Those extant activities can be inhibited by nucleotides, with low affinity (*15*, *19*), and inactivated by TNP-8N_3-ADP with a K_{TNP-8N_3-ADP} of 15−40 μM (Figure 5 and ref *18*) or by Co(NH_3)$_4$ATP with a $K_{Co(NH_3)_4ATP}$ of 0.4−0.6 mM (*44*). All this seems to signal the presence of a distinct low-affinity nucleotide site on the α-chain of FITC-modified Na,K-ATPase. This notion is supported by several enzymological criteria. (i) The low-affinity nucleotide effects are inherent to the αβ protomers of the FITC-modified (*15*, *18*) or native enzymes (*14*), so there is no need to summon a diprotomeric or higher-order structure. (ii) The FITC-labeled enzyme can bind, with low affinities, ATP, TNP-ATP, Co(NH_3)$_4$ATP, ADP, TNP-ADP, and TNP-8N_3-ADP but not AMP, while GTP, CTP, ITP, and TNP-UTP are poorer ligands (*15*, *18*−*20*, *44*). (iii) After a comprehensive block of one ATP site by FITC, Na,K-ATPase will still incorporate approximately 1 mol of TNP-8N_3-ADP per mole of α-subunit (*20*). (iv) This incorporation of TNP-8N_3-ADP is accompanied by a proportional loss of extant E2 enzymic activity (*20*). (v) Na^+ binding, presumably in the transmembrane domain, alters the properties of this nucleotide site, causing an increase in binding affinity and reactivity toward TNP-8N_3-ADP (Figure 5). (vi) Vanadate and strophanthidin, two inhibitors working from opposite sides of the membrane, lock and protect the site, preventing TNP-8N_3-ADP photoinactivation and labeling of the FITC-enzyme (*20*). The nucleotide binding that we observe in the FITC-modified Na,K-ATPase, therefore, displays properties that would be considered regulatory in nature were this a fully competent enzyme; however, the low-affinity nucleotide effects on E2 partial reactions can also be oberved in the absence of FITC treatment (*10*, *11*, *13*, *19*, *44*, *45*) where, in addition, the prominent acceleration of the Na,K-ATPase activity is enabled (*13*, *14*). It then seems reasonable to hypothesize that the high- and low-affinity ATP effects on the native sodium pump arise, at least in part, from nucleotide interactions at two distinct binding sites on the α-chain. The different TNP-8N_3-ADP anchoring sequences in native and FITC-modified Na,K-ATPase (Figures 9 and 11), labeled with different affinities, seem to shore up this view.

N-Domain Binding Site. Our affinity labeling results with native Na,K-ATPase (Figure 9) place TNP-8N_3-ATP in the N-domain, with an *anti* adenine conformation (*46*), as with 8N_3-ATP (*35*). In the case of SERCA, TNP-AMP and AMP-PCP also adopt an *anti* conformation in the high-resolution structures (*23*, *42*), and so must TNP-8N_3-ATP and TNP-8N_3-AMP before inactivation (*37*). In yeast H^+-ATPase (*47*), however, 2N_3-ATP and 2N_3-AMP label the peptide ^{560}D...K^{566}, equivalent to the *s*^{627}D...A^{632} fragment in SERCA's P-domain (*21*, *22*). Given the sequence homology, this suggests that the yeast H^+-ATPase must adopt a closed conformation (*41*, *42*) before a residue is suitably aligned for nitrene attack.

Site-directed mutagenesis has shown that αLys480 is not essential for binding of ATP to Na,K-ATPase (*48*), yet this residue is the target of several probes. In fact, H_2DIDS cross-links αLys480 to αLys501 (*49*), as DIDS does with the homologous *s*Lys492 and *s*Lys515 (*50*). Glutaraldehyde makes a zero-distance cross-link between *s*Lys492 and *s*Lys678 of SERCA's P-domain (*51*), indeed a consequence of the closure of N- and P-domains (*41*, *42*). PLP and AP_2-PL also react with αLys480 (*36*) and *s*Lys492 (*52*); ATP phosphorylation and the Na,K-ATPase activity are inactivated up to 80% (*36*), but AP_2PL has little or no effect on the K^+-phosphatase activity or P_i phosphorylation (*36*, *52*). This supports the idea that reactions at the P-domain may have considerable independence from events at the N-domain. In some cases (*50*, *53*), however, some covalent probes that bind to the N-domain also interfere with E2 functions, and this has been interpreted as evidence of a single nucleotide site. An equally plausible explanation is that spontaneous, nonproductive conformational fluctuations (*54*) result in random closure of N-, A- ("actuator"), and P-domains. In this case, bulky N-domain labels are likely to cause steric hindrance to E2 ligand binding or catalytic transactions (e.g., K^+-phosphatase reaction or P_i

Table 1: Sequence Homology of the P-Domain Peptide[a]

	position	*	**		**	**	*	**			**	**	**			**	**	position
Na,K-ATPase (pig, lamb)	721	A	D	I	G	V	A	M	G	I	A	G	S	D	V	S	K	736
H,K-ATPase (rat, dog)	737	A	D	I	G	V	A	M	G	I	A	G	S	D	A	A	K	752
PMCA 1 (rat)	805	A	D	V	G	F	A	M	G	I	A	G	T	D	V	A	K	820
SERCA 1a (rabbit)	714	A	E	I	G	I	A	M	G	-	S	G	T	A	V	A	K	728
H-ATPase (yeast)	645	A	D	T	G	I	A	V	E	-	G	A	T	D	A	A	R	659
K-ATPase (*Escherichia coli*)	529	A	D	V	A	V	A	M	N	-	S	G	T	Q	A	A	K	543
			←			*β*		→					←		α		(→)	

[a] One asterisk denotes identical residues, and two asterisks denote conservative replacement. Predicted (*21*, *22*) or actual (*23*) *β*-strand and α-helix structures are denoted as *β* and α, respectively. Data from refs *21*−*23*.

phosphorylation) that may mainly require the P-domain and, presumably, a vacant N-domain. The lack of interference of FITC with E2 reactions may simply reflect a more compact occupation of the N-domain pocket. Other aspects of some of those results (*53*) have been discussed previously (*44*).

P-Domain Sequence. Considering the results that we now report for the native enzyme (Figure 1), the photoinactivation and labeling of the FITC-modified enzyme (*18*, *20*) occur with a >100 times lower TNP-8N_3-ADP affinity (cf. Figure 5). Controlled trypsinolysis of the ^{32}P-labeled, FITC-modified Na,K-ATPase showed that TNP-8N_3-[α-^{32}P]ADP was incorporated into the C-terminal 57 kDa fragment of the α-subunit (*20*), downstream of αArg438 (*55*).

Following TNP-8N_3-[α-^{32}P]ADP labeling of FITC-modified Na,K-ATPase, the first chromatography all but failed to show the radioactive peaks that led to the α^{470}IVEI...K^{487} sequence with the native enzyme. Instead, the FITC-modified α-chain twice returned the sequence α^{721}ADIGVA...K^{736} (Figure 11), located within the C-terminal 57 kDa fragment. The peptides were clearly associated with the TNP-8N_3-[α-^{32}P]ADP radioactivity (e.g., Figure 10C), but none of the Edman cycles was unambiguously void. A coincidental C_4 elution of free radioactive probe and unlabeled α^{721}ADIGVA...K^{736} peptide seems quite unlikely. This is because we would have to assume that twice did the same fortuitous event occur in the source material [i.e., C_{18} fractions 53 in Figure 10B and 69 and 70 (peak B, not shown) in the second experiment]. We need to consider the fact that the two C_{18} runs were done with different gradients, that the relevant C_{18} peaks appeared at different times (53 and 69−70 min), and that the C_{18} and C_4 separations were done with different starting solvents and at different pHs. By far the most likely explanation is that there is a progressive release of the radioactive probe during the successive Edman cycles (*38*), with regeneration of the amino acyl residue. Similarly unstable nitrene adducts have been found (*35*, *39*, *47*).

As shown in Table 1, the α^{721}ADIGVA...K^{736} sequence is located in a highly conserved region of the large cytoplasmic loop (*21*, *22*), a homology that extends to transmembrane helix M5. At its N-terminus, this peptide is flanked by residues derivatized by other ATP affinity labels. αLys719 is an anchoring site for FSBA (*56*), while αAsp710 and αAsp714 are covalently labeled with ClR-ATP (*57*). In the case of SERCA, high-affinity ATP binding within the N-domain already occurs in the open conformation (*23*, *58*) and is followed by closure of A-, N-, and P-domains (*41*, *42*). In the closed SERCA structure containing bound AMP-PCP, aspartyls homologous to those above contribute to the stabilizing and locking of the phosphate chain (*42*). Those residues are mostly in loops issuing from *β*-strands 1, 4, and 5 of a parallel *β*-sheet that cuts through the P-domain (see Figure 5 of ref *23* and Figures 4 and 5 of ref *42*). Together with Pα5 and Pα6, they form a Rossman fold which, in the closed SERCA structures (*41*, *42*), is found in the proximity of the N-domain. However, our α^{721}ADIGVA...K^{736} sequence (Figure 11) maps onto SERCA's s^{714}AEIGIA...K^{728} tryptic fragment (*21*). This spans downstream elements in the same *β*-sheet, including most of P*β*6 and Pα7, and the connecting loop (Table 1). Jointly with P*β*7, they constitute a second Rossman fold in the P-domain (*22*, *23*, *42*). It is conceivable that this structural element might be involved in low-affinity nucleotide binding in P-type ATPases. While only one bound nucleotide has so far been detected in SERCA crystal structures (*23*, *42*), there is evidence for two ATP sites from careful TNP-ATP and TNP-AMP binding studies (*59*, *60*). In the case of H,K-ATPase, 2 mol of TNP-ATP is bound per phosphorylation site, with similar affinities (*61*); ATP, however, competes with two association constants differing by a factor of >300.

Cation Effects. When it comes to TNP-8N_3-ADP inactivation, native and FITC-modified Na,K-ATPases respond to Na^+ (and K^+) in strikingly different ways (Figure 4), yet both enzymes are known to adopt an E1 conformation in the absence of sodium ions (*16*). The conventional "Na^+" and "K^+" forms lead to distinct patterns of trypsin attack (*62*), can be observed from intrinsic fluorescence enhancements (*63*), or quench the fluorescence of covalently bound FITC (*16*, *17*, *64*). Work with Na,K-ATPase reconstituted in artificial vesicles has confirmed that the cation sites involved in these actions have an intracellular orientation (*64*). The K^+ form (c below), therefore, is being reached through partial reversal of the final sodium pump steps

$$\underset{\text{(a)}}{\text{E1}} \overset{+nK^+_{(i)}}{\rightleftharpoons} \underset{\text{(b)}}{\text{E1}\cdot K^+_n} \rightleftharpoons \underset{\text{(c)}}{\text{E2}(K^+)_n} \qquad (1)$$

starting from the E1 (a) or Na^+ form. In the absence of Na^+, internal K^+ binds at equilibrium to form an $E1\cdot K^+_n$ complex (b) that is rapidly converted into an occluded $E2(K^+)_n$ conformer (c) (*10*, *11*). The b−c step is the conformational change, heavily biased toward the right (*65*). In our experiments, we may consider this conformational transition at equilibrium, as the deocclusion rate (c → b, slow at submicromolar nucleotide concentrations) is still >100 times faster than the TNP-8N_3-ADP photoinactivation (*10*, *11*). The apparent affinity for K^+ binding in eq 1 (*66*) is then derived from the relation $K_K' = K_K/(1 + K_c) = 12\ \mu$M (Figure 4A; cf. refs *12* and *67*), where K_K is the K^+ dissociation constant

(b → a step) and K_c is the equilibrium constant[2] for the b−c step. The apparent Na^+ binding affinity should then be derived from the relation $K_{Na}' = K_{Na}(1 + [K^+]/K_K')$, and under the conditions and results in panels A and B of Figure 4, $K_{Na} = 0.17$ mM. This is comparable to the K_{Na} of 0.19 mM at each of three intracellular Na^+ sites in red cells (*68*) and to K_{Na} in the native kidney enzyme (*12*, *66*); it is also quite close to the K_{Na} in fluorescence quench experiments with the FITC-modified Na,K-ATPase (*17*). Therefore, even though our purified preparations consist of broken membranes, all this strongly suggests that the TNP-8N_3-ADP inactivation of the native enzyme is modulated by Na^+ and K^+ binding at sites with an intracellular conformation.

With regard to the FITC-modified enzyme, it is now plain that the low-affinity Na^+ requirement for TNP-8N_3-ADP inactivation is not absolute and that it operates through a combination of binding and reactivity enhancements at the nucleotide pocket (Figure 5). It also emphasizes that the increased TNP-8N_3-ADP affinity at high Na^+ concentrations (Figure 5), in addition to earlier evidence (*18*, *20*), makes the hypothesis (*69*) untenable that while the tethered FITC blocks a unique ATP site in the presence of Na^+, it moves to one side allowing nucleotide access in the presence of K^+. The quandary is that $K_{0.5(Na)}$ for TNP-8N_3-ADP inactivation of the FITC-modified enzyme (inset in Figure 4B) is 170−500-fold higher than that which can be derived from fluorescence shifts of the bound FITC (*17*, *64*) and in the range of affinities for extracellular Na^+ sites [$K_{Na,out} = 27-100$ mM (*68*, *70*)]. The hyperbolic dependence (*20*, *71*) suggested a single Na^+ binding event and probably reflects the fact that the three Na^+ ions are released to the outside medium sequentially, with decreasing rate constants (*72*, *73*). The SERCA structure (*23*, *41*, *42*) and a homology model for Na,K-ATPase (*74*) show a single set of cation sites alternating between internal and external presentations. If we now imagine steps involving external (o) cation binding without intervention of a phosphoenzyme, we could form $E2(K^+)_n$ from external K^+, subject to external Na^+ competition:

$$\underset{(c)}{E2(K^+)_n} \rightleftarrows \underset{(d)}{E2{\cdot}K^+} \underset{+K^+_{(o)}}{\rightleftharpoons} \underset{(e)}{E2} \overset{+Na^+_{(o)}}{\rightleftharpoons} \underset{(f)}{E2{\cdot}Na^+} \qquad (2)$$

Our hypothesis, therefore, is that the FITC-modified Na,K-ATPase can slowly translocate its monovalent cation sites, either loaded or unloaded, in the absence of reverse P_i phosphorylation (a−e and back, eqs 1 and 2). This has been proposed previously (*75*), in connection with the native enzyme, to account for Rb^+ and Na^+ fluxes in the absence of nucleotides and P_i. The slowest rate constant was 0.01 s^{-1} for the E1 → E2 transition with vacant cation sites at 20 °C (*75*). This only represents ≈0.02% of the maximal Na,K-ATPase turnover but is 15 times faster than the rate of TNP-8N_3-ADP photoinactivation of the FITC-modified enzyme [$k_{x(max)} = 0.041$ min^{-1}; Figure 5], which is more than adequate to allow for our results. A "relaxed carrier" behavior would explain why, at high Na^+ concentrations, the FITC-modified enzyme is not simply trapped in $E1{\cdot}Na^+_n$ conformations but can also display cation sites with an external presentation. This is because irreversible TNP-8N_3-ADP binding will pull the overall equilibrium to the right (a−f, eqs 1 and 2).

Neither the Na^+ requirement nor K^+ protection is absolute (Figures 3 and 5 and ref *20*). This agrees with the fact that the occluded K^+ form does bind ATP or ADP, with low affinity, in the presence (*9*, *11*) or absence of Na^+ (*10*, *76*, *77*). Nonetheless, the affinity of a regulatory ATP site, and hence the overall pump rate, may be under allosteric control by external Na^+ and K^+. Under turnover conditions, this is likely to be obscured by the prominent activating "substrate" action of external K^+, external Na^+ then acting as an inhibitor (*71*).

[2] Assuming that $K_K = 9-10$ mM for the equilibrium a−b binding step (refs *17* and *68*), $K_c \approx K_K/K_K' \approx 800$ under our conditions.

ACKNOWLEDGMENT

We thank Prof. C. R. Bagshaw, Dr. P. C. E. Moody, and Dr. I. G. Barsukov (Department of Biochemistry) for helpful discussions and Dr. S. Mistry (Protein and Nucleic Acid Laboratory) for help with the Edman degradations. J.D.C. dedicates this paper to Dr. Arieh Lew (Physiological Laboratory, University of Cambridge) in recognition of his selfless advice and hospitality at a very early stage.

REFERENCES

1. Kaplan, J. H. (2002) Biochemistry of Na,K-ATPase, *Annu. Rev. Biochem. 71*, 511−535.
2. Jørgensen, P. L., Håkansson, K. O., and Karlish, S. J. D. (2003) Structure and mechanism of Na,K-ATPase. Functional sites and their interactions, *Annu. Rev. Physiol. 65*, 817−849.
3. Beaugé, L. A., and DiPolo, R. (1979) Vanadate selectively inhibits the K_0^+-activated Na^+ efflux in squid axons, *Biochim. Biophys. Acta 551*, 220−223.
4. Sachs, J. R. (1980) The order of release of sodium and addition of potassium in the sodium−potassium pump reaction mechanism, *J. Physiol. 302*, 219−240.
5. Eisner, D. A., and Richards, D. E. (1981) The interaction of potassium ions and ATP on the sodium pump of resealed ghosts, *J. Physiol. 319*, 403−418.
6. Hegyvary, C., and Post, R. L. (1971) Binding of adenosine triphosphate to sodium and potassium ion-stimulated adenosine triphosphatase, *J. Biol. Chem. 246*, 5234−5240.
7. Nørby, J., and Jensen, J. (1971) Binding of ATP to brain microsomal ATPase. Determination of the ATP-binding capacity and the dissociation constant of the enzyme-ATP complex as a function of K^+ concentration, *Biochim. Biophys. Acta 233*, 104−116.
8. Mårdh, S., and Post, R. L. (1977) Phosphorylation from adenosine triphosphate of sodium- and potassium-activated adenosine triphosphatase. Comparison of enzyme-ligand complexes as precursors to the phosphoenzyme, *J. Biol. Chem. 252*, 633−638.
9. Post, R. L., Hegyvary, C., and Kume, S. (1972) Activation by adenosine triphosphate in the phosphorylation kinetics of sodium and potassium ion transport adenosine triphosphatase, *J. Biol. Chem. 247*, 6530.
10. Glynn, I. M., and Richards, D. E. (1982) Occlusion of rubidium ions by the sodium−potassium pump: Its implications for the mechanism of potassium transport, *J. Physiol. 330*, 17−43.
11. Forbush, B., III (1987) Rapid release of ^{42}K and ^{86}Rb from an occluded state of the Na,K-pump in the presence of ATP and ADP, *J. Biol. Chem. 262*, 11104−11115.
12. González-Lebrero, R. M., Kaufman, S. B., Garrahan, P. J., and Rossi, R. C. (2002) The occlusion of Rb^+ in the Na^+/K^+-ATPase. II. The effects of Rb^+, Na^+, Mg, or ATP on the equilibrium between free and occluded Rb^+, *J. Biol. Chem. 277*, 5922−5928.
13. Glynn, I. M. (1985) The Na^+,K^+-transporting adenosine triphosphatase, in *The Enzymes of Biological Membranes* (Martonosi, A. N., Ed.) Vol. 3, pp 35−114, Plenum Press, New York.
14. Ward, D. G., and Cavieres, J. D. (1993) Solubilized $\alpha\beta$ Na,K-ATPase remains protomeric during turnover yet shows apparent negative cooperativity toward ATP, *Proc. Natl. Acad. Sci. U.S.A. 90*, 5338−5336.

15. Ward, D. G., and Cavieres, J. D. (1996) Binding of 2′(3′)-*O*-(2,4,6-trinitrophenyl)ADP to soluble $\alpha\beta$ protomers of Na,K-ATPase modified with fluorescein isothiocyanate: Evidence for two distinct nucleotide sites, *J. Biol. Chem. 271*, 12317−12321.
16. Karlish, S. J. D. (1980) Characterization of conformational changes in (Na,K)ATPase labeled with fluorescein at the active site, *J. Bioenerg. Biomembr. 12*, 111−136.
17. Faller, L. D., Díaz, R. A., Scheiner-Bobis, G., and Farley, R. A. (1991) Temperature dependence of the rates of conformational changes reported by fluorescein 5′-isothiocyanate modification of H^+,K^+- and Na^+,K^+-ATPases, *Biochemistry 30*, 3503−3510.
18. Ward, D. G., and Cavieres, J. D. (1998) Photoinactivation of FITC-modified Na,K-ATPase by TNP-8N_3-ATP. Abolition of E1 and E2 partial reactions by sequential block of high and low-affinity nucleotide sites, *J. Biol. Chem. 273*, 14277−14284.
19. Scheiner-Bobis, G., Antonipillai, J., and Farley, R. A. (1993) Simultaneous binding of phosphate and TNP-ADP to FITC-modified Na^+,K^+-ATPase, *Biochemistry 32*, 9592−9599.
20. Ward, D. G., and Cavieres, J. D. (1998) Affinity labeling of two nucleotide sites on Na,K-ATPase using 2′(3′)-*O*-(2,4,6-trinitrophenyl)8-azidoadenosine 5′-[α-^{32}P]-diphosphate (TNP-8N_3-[α-^{32}P]-ADP) as a photoactivatable probe. Label incorporation before and after blocking the high affinity ATP site with fluorescein isothiocyanate, *J. Biol. Chem. 273*, 33759−33765.
21. Green, N. M. (1989) ATP-driven cation pumps: Alignment of sequences, *Biochem. Soc. Trans. 17*, 970−972.
22. Stokes, D. L., and Green, N. M. (2000) Modeling a dehalogenase fold into the 8-Å density map for Ca^{2+}-ATPase defines a new domain structure, *Biophys. J. 78*, 1765−1776.
23. Toyoshima, C., Nakasako, M., Nomura, H., and Ogawa, H. (2000) Crystal structure of the calcium pump of sarcoplasmic reticulum at 2.6 Å resolution, *Nature 405*, 647−655.
24. Jørgensen, P. L. (1974) Purification and characterization of (Na^++K^+)-ATPase. III. Purification from the outer medulla of mammalian kidney after selective removal of membrane components by sodium dodecylsulphate, *Biochim. Biophys. Acta 356*, 36−52.
25. Seebregts, C. J., and McIntosh, D. B. (1989) 2′,3′-*O*-(2,4,6-Trinitrophenyl)-8-azido mono-, di-, and triphosphates as photoaffinity probes of the Ca^{2+}-ATPase of sarcoplasmic reticulum, *J. Biol. Chem. 264*, 2043−2052.
26. Fiske, C. H., and Subbarow, Y. (1925) The colorimetric determination of phosphorus, *J. Biol. Chem. 66*, 375−400.
27. Smith, P. K., Krohn, R. I., Hermanson, G. T., Mallia, A. K., Gartner, F. H., Provenzano, M. D., Fujimoto, E. K., Goeke, N. M., Olson, B. J., and Klenk, D. C. (1985) Measurement of protein using bicinchoninic acid, *Anal. Biochem. 150*, 76−85.
28. Laemmli, U. K. (1970) Cleavage of structural proteins during the assembly of the head of bacteriophage T4, *Nature 227*, 680−685.
29. Schägger, H., and von Jagow, G. (1987) Tricine-sodium dodecyl sulfate-polyacrylamide gel electrophoresis for the separation of protein in the range from 1 to 100 kDa, *Anal. Biochem. 166*, 368−379.
30. Kitz, R., and Wilson, I. B. (1962) Esters of methanesulfonic acid as irreversible inhibitors of acetylcholinesterase, *J. Biol. Chem. 237*, 3245−3249.
31. Moczydlowsky, E. G., and Fortes, P. A. G. (1981) Characterization of 2′,3′-*O*-(2,4,6-trinitrocyclohexadienylidine)adenosine 5′-triphosphate as a fluorescent probe of the ATP site of sodium and potassium transport adenosine triphosphatase. Determination of nucleotide binding stoichiometry and ion-induced changes in affinity for ATP, *J. Biol. Chem. 256*, 2346−2356.
32. Scheiner-Bobis, G., and Schoner, W. (1985) Demonstration of an Mg^{2+}-induced conformational change by photoaffinity labelling of the high-affinity ATP-binding site of (Na^++K^+)-ATPase with 8-azido-ATP, *Eur. J. Biochem. 152*, 739−746.
33. Skou, J. C., and Esmann, M. (1983) Effect of magnesium ions on the high-affinity binding of eosin to the (Na^++K^+)-ATPase, *Biochim. Biophys. Acta 727*, 101−107.
34. Ovchinnikov, Y. A., Modyanov, N. N., Broude, N. E., Petrukhin, K. E., Grishin, A. V., Arzamazova, N. M., Aldanova, N. A., Monastyrskaya, G. S., and Sverdlov, E. D. (1986) Pig kidney Na^+,K^+-ATPase primary structure and spatial organisation, *FEBS Lett. 201*, 237−245.
35. Tran, C. M., Scheiner-Bobis, G., Schoner, W., and Farley, R. A. (1994) Identification of an amino acid in the ATP binding site of Na^+/K^+-ATPase after photochemical labeling with 8-azido-ATP, *Biochemistry 33*, 4140−4147.
36. Kaya, S., Tsuda, T., Hagiwara, K., Fukui, T., and Taniguchi, K. (1994) Pyridoxal 5′-phosphate probes at Lys-480 can sense the binding of ATP and the formation of phosphoenzymes in Na^+,K^+-ATPase, *J. Biol. Chem. 269*, 7419−7422.
37. McIntosh, D. B., Woolley, D. G., and Berman, M. C. (1992) 2′,3′-*O*-(2,4,6-Trinitrophenyl)-8-azido-AMP and -ATP photolabel Lys-492 at the active site of sarcoplasmic reticulum Ca^{2+}-ATPase, *J. Biol. Chem. 267*, 5301−5309.
38. Allen, G. (1981) *Sequencing of Proteins and Peptides*, North-Holland, Amsterdam.
39. Tran, C. M., Huston, E. E., and Farley, R. A. (1994) Photochemical labeling and inhibition of Na,K-ATPase by 2-azido-ATP. Identification of an amino acid located within the ATP binding site, *J. Biol. Chem. 269*, 6558−6565.
40. Farley, R. A., Tran, C. M., Carilli, C. T., Hawke, D., and Shively, J. E. (1984) The amino acid sequence of a fluorescein-labeled peptide from the active site of (Na,K)-ATPase, *J. Biol. Chem. 259*, 9532−9535.
41. Toyoshima, C., Nomura, H., and Tsuda, T. (2004) Lumenal gating mechanisms revealed in calcium pump crystal structures with phosphate analogues, *Nature 432*, 361−368.
42. Toyoshima, C., and Mizutani, T. (2004) Crystal structure of the calcium pump with a bound ATP analogue, *Nature 430*, 529−535.
43. Mitchinson, C., Wilderspin, A. F., Trinnaman, B. J., and Green, N. M. (1982) Identification of a labelled peptide after stoicheiometric reaction of fluorescein isothiocyanate with the Ca^{2+}-dependent adenosine triphosphatase of sarcoplasmic reticulum, *FEBS Lett. 146*, 87−92.
44. Ward, D. G., and Cavieres, J. D. (2003) Inactivation of Na,K-ATPase following $Co(NH_3)_4$ATP binding at a low affinity site in the protomeric enzyme unit, *J. Biol. Chem. 278*, 14688−14697.
45. Robinson, J. D. (1976) Substrate sites in the (Na^++K^+)-dependent ATPase, *Biochim. Biophys. Acta 429*, 1006−1019.
46. Scheit, K. H. (1980) *Nucleotide Analogs. Synthesis and Biological Function*, p 7, John Wiley & Sons, New York.
47. Davis, C. B., Smith, K. E., Campbell, B. N., Jr., and Hammes, G. G. (1990) The ATP binding site of the yeast plasma membrane proton-translocating ATPase, *J. Biol. Chem. 265*, 1300−1305.
48. Wang, K., and Farley, R. A. (1992) Lysine 480 is not an essential residue for ATP binding or hydrolysis by Na,K-ATPase, *J. Biol. Chem. 267*, 3577−3580.
49. Gatto, C., Lutsenko, S., and Kaplan, J. H. (1997) Chemical modification with dihydro-4,4′-diisothiocyanostilbene-2,2′-disulfonate reveals the distance between K_{480} and K_{501} in the ATP-binding domain of the Na,K-ATPase, *Arch. Biochem. Biophys. 340*, 90−100.
50. Hua, S., Ma, H., Lewis, D., Inesi, G., and Toyoshima, C. (2002) Functional role of "N" (nucleotide) and "P" (phosphorylation) domain interactions in the sarcoplasmic reticulum (SERCA) ATPase, *Biochemistry 41*, 2264−2272.
51. McIntosh, D. B. (1992) Glutaraldehyde cross-links Lys-492 and Arg-678 at the active site of sarcoplasmic reticulum Ca^{2+}-ATPase, *J. Biol. Chem. 267*, 22328−22335.
52. Tsuda, T., Kaya, S., Funatsu, H., Hayashi, Y., and Taniguchi, K. (1998) Fluorescein 5′-isothiocyanate-modified Na^+,K^+-ATPase, at Lys-501 of the α-chain, accepts ATP independent of pyridoxal 5′-diphospho-5′-adenosine modification at Lys-480, *J. Biochem. 123*, 169−174.
53. Martin, D., and Sachs, J. R. (2000) Ligands presumed to label high affinity and low affinity ATP binding sites do not interact in an $(\alpha\beta)_2$ diprotomer in duck nasal gland Na^+,K^+-ATPase, nor do the sites coexist in native enzyme, *J. Biol. Chem. 275*, 24512.
54. Eizenmesser, E. Z., Millet, O., Labeikovsky, W., Korzhenev, D. M., Wolf-Watz, M., Bosco, D. A., Skalicky, J. J., Kay, L. A., and Kern, D. (2005) Intrinsic dynamics of an enzyme underlies catalysis, *Nature 438*, 117−122.
55. Jørgensen, P. L., and Collins, J. H. (1986) Tryptic and chymotryptic cleavage sites in sequence of α-subunit of (Na^++K^+)-ATPase from outer medulla of mammalian kidney, *Biochim. Biophys. Acta 860*, 570−576.
56. Ohta, T., Nagano, K., and Yoshida, M. (1986) The active site structure of Na^+/K^+-transporting ATPase: Location of the 5′-(*p*-fluorosulfonyl)bezoyladenosine binding site and soluble peptides released by trypsin, *Proc. Natl. Acad. Sci. U.S.A. 83*, 2071−2075.
57. Ovchinnikov, Y. A., Dzhandzugazyan, K. N., Lutsenko, S. V., Mustayev, A. A., and Modyanov, N. N. (1987) Affinity modification of E1-form of Na^+,K^+-ATPase revealed Asp-710 in the catalytic site, *FEBS Lett. 217*, 111−116.

58. Ma, H., Inesi, G., and Toyoshima, C. (2003) Substrate-induced conformational fit and headpiece closure in the Ca^{2+}-ATPase (SERCA), *J. Biol. Chem. 278*, 28938−28943.
59. Watanabe, T., and Inesi, G. (1982) The use of 2′,3′-*O*-(2,4,6-trinitrophenyl) adenosine 5′-triphosphate for studies of nucleotide interaction with sarcoplasmic reticulum vesicles, *J. Biol. Chem. 257*, 11510−11516.
60. Suzuki, H., Kubota, T., Kubo, K., and Kanazawa, T. (1990) Existence of a low-affinity ATP-binding site in the unphosphorylated Ca^{2+}-ATPase of sarcoplasmic reticulum vesicles: Evidence from binding of 2′,3′-*O*-(2,4,6-trinitrocyclohexadienylidene)-[^{3}H]-AMP and -[^{3}H]ATP, *Biochemistry 29*, 7040−7045.
61. Faller, L. D. (1989) Competitive binding of ATP and the fluorescent substrate analogue 2′,3′-*O*-(2,4,6-trinitrophenylcyclohexadienylidine)adenosine 5′-triphosphate to the gastric H^+,K^+-ATPase: Evidence for two classes of nucleotide sites, *Biochemistry 28*, 6771−6778.
62. Jørgensen, P. L. (1975) Purification and characterization of (Na^+,K^+)-ATPase. V. Conformational changes in the enzyme transitions between the Na-form and the K-form studied with tryptic digestion as a tool, *Biochim. Biophys. Acta 401*, 399−415.
63. Karlish, S. J. D., and Yates, D. W. (1978) Tryptophan fluorescence of (Na^++K^+)-ATPase as a tool for study of the enzyme mechanism, *Biochim. Biophys. Acta 527*, 115−130.
64. Rephaeli, A., Richards, D., and Karlish, S. J. D. (1986) Conformational transitions in fluorescein-labeled (Na,K)ATPase reconstituted into phospholipid vesicles, *J. Biol. Chem. 261*, 6248−6254.
65. Karlish, S. J. D., Yates, D. W., and Glynn, I. M. (1978) Elementary steps of the (Na^++K^+)-ATPase mechanism, studied with formycin nucleotides, *Biochim. Biophys. Acta 525*, 230−251.
66. Karlish, S. J. D., Yates, D. W., and Glynn, I. M. (1978) Conformational transitions between Na^+-bound and K^+-bound forms of (Na^++K^+)-ATPase, studied with formycin nucleotides, *Biochim. Biophys. Acta 525*, 252−264.
67. González-Lebrero, R. M., Kaufman, S. B., Montes, M. R., Nørby, J., Garrahan, P. J., and Rossi, R. C. (2002) The occlusion of Rb^+ in the Na^+/K^+-ATPase. I. The identity of occluded states formed by the physiological route or the direct routes: Occlusion/deocclusion kinetics through the direct route, *J. Biol. Chem. 277*, 5910−5921.
68. Garay, R. P., and Garrahan, P. J. (1973) The interaction of sodium and potassium with the sodium pump in red cells, *J. Physiol. 231*, 297−325.
69. Davis, R. L., and Robinson, J. D. (1988) Substrate sites of the (Na^++K^+)-ATPase: Pertinence of the adenine and fluorescein binding sites, *Biochim. Biophys. Acta 953*, 26−36.
70. Kaplan, J. H. (1982) Sodium pump-mediated ATP:ADP exchange. The sided effects of sodium and potassium ions, *J. Gen. Physiol. 80*, 915−937.
71. Cavieres, J. D., and Ellory, J. C. (1975) Allosteric inhibition of the sodium pump by external sodium, *Nature 255*, 338−340.
72. Jørgensen, P. L., and Andersen, J. P. (1988) Structural basis for E_1-E_2 conformational transitions in Na,K-pump and Ca-pump proteins, *J. Membr. Biol. 103*, 95−120.
73. Holmgren, M., Wagg, J., Bezanilla, F., Rakowski, R. F., De Weer, P., and Gadsby, D. C. (2000) Three distinct and sequential steps in the release of sodium ions by the Na^+/K^+-ATPase, *Nature 403*, 898−901.
74. Ogawa, H., and Toyoshima, C. (2002) Homology modelling of the cation binding sites of Na^+K^+-ATPase, *Proc. Natl. Acad. Sci. U.S.A. 99*, 15977−15982.
75. Karlish, S. J. D., and Stein, W. D. (1982) Passive rubidium fluxes mediated by Na,K-ATPase reconstituted into phospholipid vesicles when ATP- and phosphate-free, *J. Physiol. 328*, 295−316.
76. Hasenauer, J., Huang, W.-H., and Askari, A. (1993) Allosteric regulation of the access channels to the Rb^+ occlusion sites of (Na^++K^+)-ATPase, *J. Biol. Chem. 268*, 3289−3297.
77. Liu, L., and Askari, A. (1997) Evidence for the existence of two ATP-sensitive Rb^+ occlusion pockets within the transmembrane domains of Na^+/K^+-ATPase, *J. Biol. Chem. 272*, 14380−14386.

BI051927K